Lisbon School of Economics and Management

Lévy Processes and Applications

Option Pricing with a Time-Changed Meixner Model

Group A

Eduardo Peso
56513

Martim Costa
56950

Sofia Mineiro
56910

Vasco Tavares
56512

2022/2023 - 1st Semester

Contents

Abstract

This report illustrates option pricing methods with an emphasis on stochastically changing volatility. Financial markets exhibit different behaviours which sometimes are challenging to model, among which is the fact that extreme events are more likely to happen, asset prices have jumps and fluctuate stochastically. In our project, we will take the Meixner model and subordinate it to the time integral of a Cox-Ingerssol-Ross process, which will induce stochastic volatility and volatility clustering, resulting in a Meixner-CIR process. Furthermore, our results show us that, within the different models applied, the time-changed Meixner is the one that presents better results, which is to be expected since it introduces crucial financial markets characteristics that the other models do not. These results show us that, to price financial assets, stochastic volatility is an important component, although the models that result from its inclusion are less parsimonious.

1 Introduction

Financial markets started being modelled with stochastic processes more than one hundred years ago with the pioneering work of Bachelier, who used Brownian motion with drift to model stock prices. Though Bachelier's intuition proved fruitful, it was not yet mathematically sound; for example, negative stock prices could occur in his model. Brownian motion is more manageable than any alternative process, but it is a poor approximation of financial reality. Bachelier himself was the first to notice this, but many other authors in the 1960s pointed out the discrepancies between his model and reality [5]. In that decade, geometric Brownian motion was proposed by Samuelson as an alternative to standard Brownian motion to model stock prices. One decade later, Black, Scholes, and Merton demonstrated how to price European options based on the geometric Brownian motion [8]. Their model is the celebrated Black-Scholes model, and it uses the Normal distribution to fit the log-returns of the underlying. However, this model also comes with its own flaws. Namely, we outline that the log-returns of most assets have fatter tails than that of the normal distribution [7], which gives rise to the presence of a volatility smile (implied volatilities are higher in options that are deeply in- or out-of-the-money) [4].

To tackle these issues, in the late 1980s and in the 1990s, Lévy processes started being used in Finance [8]. These are stochastic processes with independent and stationary increments and with infinitely divisible distributions. They are especially useful if these distributions feature excess kurtosis to replace the underlying Normal distribution that models stock prices. An example of such distributions is the Meixner distribution, which is presented and utilized in [7].

However, there is an important feature that is missing from these Lévy models: stochastically changing volatility. One way of incorporating a volatility effect, which we will use in this work, is to increase or decrease the level of uncertainty by speeding up or slowing down the rate at which time passes. In periods of high volatility, time will run faster than in periods of low volatility. A candidate is the classical mean-reverting Cox–Ingersoll–Ross (CIR) process, which is based on Brownian motion [8].

Therefore, in our work we will study a Stochastic Volatility (SV) model: we take the Meixner model and subordinate it to the time integral of a CIR process. The randomness of the CIR process induces SV in the model, and the mean reversion introduces volatility clustering [2]. We will refer to this process as Meixner-CIR.

This work is organized as follows: after this brief introduction, in Section 2 we introduce the Meixner distribution, Meixner process and the CIR process. Next, in Section 3 we introduce the methods for the simulations and option pricing: the implementation of the Brownian motion, Poisson process, and the

CIR and Meixner processes. That is followed by Section 4, where some trajectories are simulated for all these processes. Then, Section 5 is concerning the calculation of the price of some European call options on the S&P 500 Index at the close of the market on April 18, 2002. We will compare the results obtained via Monte Carlo simulation to those with the appropriate closed form formula, besides computing the implied volatilities by using the Black-Scholes formula. In Section 6, we will calculate the price of an exotic Barrier option of the type "down-and-in barrier call" (DIBC) as required. Last but not least, in Section 7 we conclude with the main results.

2 Implemented Models

2.1 The Meixner Process

The Meixner process was first introduced by Schoutens and Teugels, in 1998 [9], and originates from the theory of orthogonal polynomials [8]. Its applications to Finance were also worked on by Schoutens, in 2002 [7]. For the following information on this distribution, we will refer to [8] and [7].

The density of the Meixner distribution, which is written as Meixner(a, b, m, d), is given by

$$f(x; a, b, m, d) = \frac{(2\cos(b/2)^{2d}}{2a\pi\Gamma(2d)} \exp\left(\frac{b(x-m)}{a}\right) \left|\Gamma\left(d + \frac{\mathrm{i}(x-m)}{a}\right)\right|^2, \tag{2.1.1}$$

where $a > 0, -\pi < b < \pi, d > 0$, and $m \in \mathbb{R}$.

Moments of all order exist for the Meixner distribution. In particular, an important result which arises from this density is the Kurtosis of the Meixner distribution, which is equal to

$$\text{Kurtosis}(\text{Meixner}(x; a, b, m, d)) = 3 + \frac{3 - 2\cos^2(b/2)}{d}. \tag{2.1.2}$$

Clearly, the kurtosis of the Meixner distribution is always greater than 3, which is the Normal kurtosis. This is a nice feature of this distribution, as financial returns are usually leptokurtic. It can be even shown that the Meixner distribution has semiheavy tails.

Moreover, the characteristic function of the Meixner(a, b, m, d) distribution is given by

$$\phi_{\text{Meixner}}(u; a, b, m, d) = \mathbb{E}\left[e^{iuM_1}\right] = \left(\frac{\cos(b/2)}{\cosh\left(\frac{au-ib}{2}\right)}\right)^{2d} \exp(imu). \tag{2.1.3}$$

We can also write the characteristic exponent (or Lévy symbol) of this distribution:

$$\psi_X(u) = imu + \log\left[\left(\frac{\cos(b/2)}{\cosh((au-ib)/2)}\right)^{2d}\right] \tag{2.1.4}$$

With this characteristic function, we see that the Meixner(a, b, m, d) distribution is infinitely divisible. We can associate infinitely divisible distributions with Lévy processes by the Lévy-Khintchine formula, which is a result we now recall for the one-dimensional case.

Theorem 2.1.1 (Lévy-Khintchine formula)**.** *The distribution P_X of a random variable X is infinitely divisible if and only if there exists a triplet (γ, c, ν) where $\gamma \in \mathbb{R}$, $c \geq 0$ and ν is a Lévy measure on*

$\mathbb{R} - \{0\}$ *such that, for all* $u \in \mathbb{R}$,

$$\mathbb{E}\left[e^{iuX}\right] = \exp\left[i\gamma u - \frac{u^2 c}{2} + \int_{\mathbb{R}-\{0\}} \left(e^{iux} - 1 - iux\mathbf{1}_{\{|x|<1\}}\right)\nu(dx)\right]. \tag{2.1.5}$$

Therefore, we can associate this distribution with a Lévy process which we call the Meixner process.

Definition 2.1.1 (*Meixner Process*)**.** The Meixner process $\{M_t, t \geq 0\}$ is a stochastic process which starts at zero, i.e. $M_0 = 0$, has independent and stationary increments, and where the distribution of M_t is given by the Meixner distribution Meixner(a, b, mt, dt).

In general, a Lévy process consists of three independent parts: a drift part, a Brownian part, and a pure jump part. The Meixner process has no Brownian part, and its jumps are governed by the Lévy measure:

$$\nu(dx) = d \cdot \frac{\exp(bx/a)}{x \sinh(\pi x/a)}\, dx. \tag{2.1.6}$$

One can show that this process has infinite variation. Moreover, the first parameter in the Lévy triplet (see 2.1.5) is equal to

$$\gamma = m + ad\tan(b/2) - 2d\int_1^\infty \frac{\sinh(bx/a)}{\sinh(\pi x/a)}\, dx. \tag{2.1.7}$$

This will be especially useful for the simulation of the trajectories of this process.

2.2 The Cox-Ingersoll-Ross Process

The CIR process, also known as the square root process, is a one-factor equilibrium model that was introduced in 1985 by John C. Cox, Jonathan E. Ingersoll and Stephen A. Ross as an extension of the Vasicek model (the first model to describe the evolution of interest rates while expressing mean reversion). When applied to mathematical finance, the model describes the evolution of interest rates, outlining interest rate movements when affected by a single source of risk. The process is a common tool when forecasting interest rates in bond pricing models. It is defined as the process that solves the following stochastic differential equation:

$$\mathrm{d}y_t = \kappa\left(\eta - y_t\right)\mathrm{d}t + \lambda y_t^{1/2}\, \mathrm{d}W_t, \tag{2.2.1}$$

where $W = \{W_t, t \geq 0\}$ represents a standard Brownian motion. The parameters κ, η, λ are positive constants and represent the long-run rate of time, the rate of mean reversion and volatility of the time change, respectively. The drift factor, $\kappa\left(\eta - y_t\right)$, is the same as in Vasicek model, being that ensures the mean reversion of the interest rate. The standard deviation factor, $\lambda y_t^{1/2}$, usually guarantees the nonexistence of negative interest rates [8]. The following proposition ensures us of the condition for only obtaining positive values for y_t [1].

Proposition 2.2.1. *Assume that* $y(0) > 0$*. If* $2\kappa\eta \geq \lambda^2$*, then the process for* y *can never reach zero. If* $2\kappa\eta < \lambda^2$*, then the origin is accessible and strongly reflecting.*

The condition $2\kappa\eta \geq \lambda^2$ in Proposition 2.2.1 is known as the *Feller condition*. We call the reader's attention to the fact that, when (2.2.1) represents a stochastic variance process, the Feller condition rarely holds. This may increase the difficulty of the Monte Carlo path generation considerably [1].

A particular limitation of this model is its high sensitivity to the parameters chosen by the person operating it. This is especially important when the volatility of the period extends beyond the parameters initially selected which restricts the scope and reliability of the process.

2.2.1 The Integrated Cox-Ingersoll-Ross Process

The integrated CIR process represents the economic time elapsed in t units of calendar time, and is simply:

$$Y_t = \int_0^t y_s \, \mathrm{d}s \tag{2.2.2}$$

When the parameters check the Feller condition, y is surely a positive process. In that case, Y_t is increasing in its domain. So, it can also be proved that it is a subordinator.

The characteristic function of Y_t will be useful in the implementation of our model. It is explicitly known [8] and it is given by:

$$\begin{aligned} \mathbb{E}\left[\exp\left(\mathrm{i}uY_t\right) \mid y_0\right] &= \varphi\left(u, t; \kappa, \eta, \lambda, y_0\right) \\ &= \frac{\exp\left(\frac{\kappa^2\eta t}{\lambda^2}\right) \exp\left(\frac{2y_0 \mathrm{i}u}{\kappa+\gamma\coth(\gamma t/2)}\right)}{[\cosh(\gamma t/2) + \kappa/\gamma \sinh(\gamma t/2)]^{2\kappa\eta/\lambda^2}}, \end{aligned} \tag{2.2.3}$$

where $\gamma = \sqrt{\kappa^2 - 2\lambda^2 iu}$.

2.3 The Meixner-CIR Process

As aforementioned, in this work we will include Stochastic Volatility by subordinating the Meixner process to the integrated CIR process. Empirical work has generally supported the need for both ingredients. Stochastic volatility appears to be needed to explain the variation in strike of option prices at longer terms, while jumps are needed to explain the variation in strike at shorter terms [8].

Throughout this work, let $Y = \{Y_t, t \geq 0\}$ be the integrated CIR process. Its characteristic function, given y_0, is denoted by $\varphi(u; t, y_0)$ and is given by eqn. (2.2.3).

Using Y as the process that models our business time, the risk-neutral price process $S = \{S_t, t \geq 0\}$ is modelled as follows:

$$S_t = S_0 \frac{\exp((r-q)t)}{\mathbb{E}\left[\exp(X_{Y_t} \mid y_0)\right]} \exp(X_{Y_t}), \tag{2.3.1}$$

where $X = \{X_t, t \geq 0\}$ is the Meixner process.

The characteristic function $\phi(u) = \phi(u; t, S_0, y_0)$ for the logarithm of our stock price is given by:

$$\begin{aligned} \phi(u) &= \mathbb{E}\left[\exp\left(\mathrm{i}u \log\left(S_t\right)\right) \mid S_0, y_0\right] \\ &= \exp\left(\mathrm{i}u\left((r-q)t + \log S_0\right)\right) \frac{\varphi\left(-\mathrm{i}\psi_X(u); t, y_0\right)}{\varphi\left(-\mathrm{i}\psi_X(-\mathrm{i}); t, y_0\right)^{\mathrm{i}u}}. \end{aligned} \tag{2.3.2}$$

This characteristic function is important in the subsequent section, where we will price some vanilla call options.

Moreover, it is noted in [2] that the expectation in eqn. (2.3.1) is simply given by:

$$\mathbb{E}\left[\exp(X_{Y_t} \mid y_0)\right] = \varphi(-i\psi_X(-i), t; \kappa, \eta, \lambda, y_0). \tag{2.3.3}$$

3 Methods for the Simulations and Option Pricing

In this subsection, we describe the methods used to implement the proposed model. To do so, we first see how to implement the Meixner and the integrated CIR processes, and later we delve into the problem of implementing the time-change by subordinating the Meixner process.

3.1 Brownian Motion and the Poisson Process

Computers deal exclusively with discrete data structures. The modelling of a continuous abstraction, such a continuous interval of real numbers, necessarily involves some concession in fidelity to the original model. The natural starting point of any such simulation is thus the approximation of the continuous by the discrete. For the Brownian motion and Poisson process, this means we have to split up the interval of time into points on which a realization of the process may be simulated.

Let Δt be a positive real number. Given that a Brownian motion W has independent and Normally distributed increments, then $W_{n\Delta t} - W_{(n-1)\Delta t} \sim \mathcal{N}(0, \Delta t)$. Let $\{v_n : n \in \mathbb{N}\}$ be a sequence of standard Normal random numbers; then, we have

$$W_0 = 0, \qquad W_{n\Delta t} = W_{(n-1)\Delta t} + \sqrt{\Delta t} v_n, \quad n \geq 1,$$

which is easily implemented in a suitable programming language.

For the Poisson process, we initially used the method of exponential spacings described in [8], but upon comparison with `Numpy`'s built-in Poisson random number generator, there was a noticeable reduction in execution time, which led us to choose it over the former algorithm. This function draws a sample from a Poisson distribution. To simulate a trajectory of a Poisson process N with intensity λ, we can consider $\{p_i : i \in \mathbb{N}\}$ Poisson random numbers with intensity $\Delta t\lambda$, our trajectory is then determined by the equations:

$$N_0 = 0, \qquad N_{n\Delta t} = N_{(n-1)\Delta t} + p_n, \quad n \geq 1.$$

3.2 Implementing the Meixner Process

The simulation of a trajectory of a Lévy process $X = \{X_t : t \geq 0\}$ with characteristic triplet $(\gamma, \sigma^2, \nu(dx))$ begins with the discretisation of ν. To this end, we fix $\varepsilon > 0$ and partition the domain of integration $\mathbb{R} \setminus [-\varepsilon, \varepsilon]$ by choosing real numbers

$$a_0 < a_1 < \cdots < a_k = -\varepsilon \text{ and } \varepsilon = a_{k+1} < a_{k+2} < \cdots < a_{d+1}.$$

Following this, we can now consider the intervals

$$[a_1, a_2), \ldots, [a_{k-1}, a_k), [a_{k+1}, a_{k+2}), \ldots, [a_d, a_{d+1}).$$

The value attributed by ν to one such interval is the probability of a jump with size between the interval's endpoints occurring. We fix a, $d \in \mathbb{N}$ and define

$$\lambda_i = \begin{cases} \nu([a_{i-1}, a_i)) & \text{for } 1 \leq i \leq k \\ \nu([a_i, a_{i+1})) & \text{for } k+1 \leq i \leq d \end{cases}.$$

Each λ_i will determine the intensity of a corresponding Poisson process $N_t^{(i)} \sim \text{Poisson}(\lambda_i)$.

Thus far, we have not specified the concrete way this partitioning is conducted, and in fact, there are different alternatives, yielding drastically different results [8]. One possibility is defining the partition uniformly, i.e. in such a way so that every interval has the same length. However, this would result in an explosion of the values λ near the origin. To counter this effect, the method we chose is the "Inverse Linear Boundaries" method, where the endpoints are given by

$$a_{i-1} = -\alpha i^{-1} \text{ and } a_{2k+2-i} = \alpha i^{-1} \qquad \text{for } 1 \leq i \leq k+1 \tag{3.2.1}$$

and some fixed $\alpha > 0$.

The original process X can now be approximated by a new process X^d defined by

$$X_t^d = \gamma t + \tilde{\sigma} W_t + \sum_{i=1}^{d} c_i (N_t^{(i)} - \lambda_i t \mathbf{1}_{|c_i|<1}) \tag{3.2.2}$$

where

$$c_i^2 \lambda_i = \begin{cases} \int_{a_{i-1}}^{a_i} x^2 \, \nu(dx) & \text{for } 1 \leq i \leq k \\ \int_{a_i}^{a_{i+1}} x^2 \, \nu(dx) & \text{for } k+1 \leq i \leq d \end{cases}.$$

and

$$\tilde{\sigma}^2 = \sigma^2 + \sigma^2(\varepsilon) = \sigma^2 + \int_{|x|<\varepsilon} x^2 \, \nu(dx).$$

For the particular case where X is the Meixner process, due to the absence of a Brownian term, we obtain simply $\tilde{\sigma}^2 = \sigma^2(\varepsilon)$.

3.3 Implementing the CIR and Integrated CIR Processes

The simulation of the CIR process $y = \{y_t, y \geq 0\}$ starts by discretising the SDE presented in eqn. (2.2.1). Thus, the sample path of the CIR process y in the time points $t = n\Delta t, n = 0, 1, 2, ...$ is given by:

$$y_{n\Delta t} = y_{(n-1)\Delta t} + \kappa(\eta - y_{(n-1)\Delta t})\Delta t + \lambda \sqrt{\Delta t y_{(n-1)\Delta t}} v_n, \tag{3.3.1}$$

where $\{v_n, n = 1, 2, ...\}$ is a series of independent standard normal random variables [8]. This is a classical and simple Euler scheme, which in this case has several drawbacks. The clearest and most known issue is that it has first-order weak convergence [1]. Yet, the most problematic feature of this discretisation is that the discrete process for y can become negative with non-zero probability, making the computation of $\sqrt{y_t}$ fail. This problem is worsened by the fact that the parameters calibrated by Schoutens and that we will use in our work do not check the Feller condition, and thus the origin is accessible (see Proposition 2.2.1). To get around this problem, it is suggested in [1] to change the discretisation to:

$$y_{n\Delta t} = y_{(n-1)\Delta t} + \kappa(\eta - y^+_{(n-1)\Delta t})\Delta t + \lambda \sqrt{\Delta t y^+_{(n-1)\Delta t}} v_n, \tag{3.3.2}$$

where $y^+ = \max\{y, 0\}$. However, this does not work for our case, because the process for y is still allowed to go below zero, after which it is forced to go to positive values again. The implementation for the CIR process would thus work, but we need that it is always non-negative. That is required because the integrated CIR process needs to be increasing to be a subordinator.

Therefore, our solution was just to take the absolute value of each point throughout the entire trajectory. Thus, the scheme for the CIR process became:

$$y_{n\Delta t} = \left| y_{(n-1)\Delta t} + \kappa(\eta - y_{(n-1)\Delta t})\Delta t + \lambda\sqrt{\Delta t y_{(n-1)\Delta t}}v_n \right|. \tag{3.3.3}$$

We are now certain that no negative values are simulated for the CIR process. Thus, the integrated CIR process will be a subordinator and it is obtained simply by the following scheme:

$$Y_{n\Delta t} = Y_{(n-1)\Delta t} + y_{n\Delta t}, \quad Y_0 = 0 \tag{3.3.4}$$

3.4 Implementing the time-changed Meixner process

With the previous subsections being about the implementation of the Meixner and the integrated CIR processes, we now see how to put them both together and subordinate the Meixner process.

We recall that the characteristic function of the Meixner-CIR process was already presented before. Now, we are interested in creating simulations where the deterministic time of the Meixner process is replaced by the integrated CIR process. The following procedure should be followed to simulate such trajectories of the stock price process $S = \{S_t, 0 \leq t \leq T\}$:

1. Simulate the CIR process $y = \{y_t, 0 \leq t \leq T\}$;
2. Calculate from the previous step the time change $Y = \{Y_t = \int_0^t y_s\, ds, 0 \leq t \leq T\}$;
3. Simulate the Meixner process $X = \{X_t, 0 \leq t \leq Y_T\}$ (noticing that we sample over $[0, Y_T]$);
4. Calculate the time-changed Meixner process X_{Y_t}, for $t \in [0, T]$;
5. Calculate the stock price $S = \{S_t, 0 \leq t \leq T\}$.

This procedure will result in a simulation of one trajectory (or sample path, a possible realization) of the time-changed Meixner process. In our project, this will be useful to perform option pricing via Monte Carlo simulations. The vanilla call options can be priced by this route, despite the existence of a closed-form formula for that case. However, Monte Carlo simulations are especially useful for the pricing of exotic options, for which there is no closed-form formula available. In this assignment, we will price a "down-and-in barrier call" (DIBC).

For the case when Monte Carlo simulations are necessary to compute the price of contingent claims, one should repeat the procedure above to simulate a significant number of sample paths of the stock price. For each path, the value of the payoff function that is associated to the contingent claim should be computed. Then, the Monte Carlo estimate of the expected value of the payoff is simply the mean of all the samples' payoffs, and the final option price is obtained by discounting this estimate.

4 Simulation of Trajectories

With the techniques presented in the previous section, we implemented our model in *Python*. We will dedicate this section to the presentation, discussion, and analysis of our implementation in what concerns the simulation of some trajectories of the processes considered here.

4.1 Preparation

4.1.1 Simulation of the Meixner Process

Simulating the Brownian motion and the Poisson process is straightforward using the procedures described in Section 3.1. The most delicate part begins in the simulation of the Meixner process. We discretize the Lévy measure $\nu(dx)$ associated to the Meixner process and we make the choice of the intervals $[a_{i-1}, a_i), i \in \{1, 2, \ldots, d\}$ with the inverse linear boundaries method, as mentioned before. This choice is crucial to ensure the numerical stability of the numerical methods employed here.

So, for the same parameters as in Schoutens's book, we plot the intensity parameters λ_i against the jump sizes c_i obtained after implementing the procedure. That comparison is in Figure A.1 (in the Appendix): Fig. A.1a depicts the intensities of the Poisson processes vs. their jump sizes in our implementation, and Fig. A.1b is the same plot with the same parameters for the Meixner process, but obtained by Schoutens in [8]. The similarity between the intensities of the Poisson processes and corresponding jump sizes simulated by us and by Schoutens in [8] indicate that this part of the implementation is not only adequate but also correct.

However, there is a small but extremely important detail that is worth mentioning at this stage. Although Schoutens's book features all the calibrated parameters for the simulations, it is not clear about the cut-off point in the discretization of the Lévy measure (the α in eqn. (3.2.1)) and the number of intervals in both sides of that partition (the k in the same equation). We started by assuming $\alpha = 0.2$ because that was the value presented in Figure A.1b, and considering that $k = 50$ would be a reasonable number of intervals for the approximation. But this turned out to be an issue in the subsequent part of our work, where we price some call options. Because of the chosen values for α and k, we were getting high errors in the computation of the price of those options. Therefore, we decided to choose the parameters $\alpha = 1$ and $k = 100$. The choice of the value of α is motivated by its interpretation in Finance: it is not possible to have a drop in the stock price of more than -100% (which would correspond to an $\alpha < -1$) and a positive jump of 100% is extremely rare. As for the choice of k, it revealed to be a good trade-off between the fit quality of our model and the time it takes to run the simulations. Moreover, to simulate the trajectories, we used 200 time points in the time discretization.

Thus, everything is set to simulate some trajectories of the Meixner process. Figure A.2 (in the Appendix) features two plots that depict twenty trajectories each, obtained by the aforementioned methods. In Figure A.2a, the utilised parameters are the ones calibrated by Schoutens, which we will use to price the call options in the next part of the work. Figure A.2b follows the same logic, but with different parameters, chosen randomly by us. It is possible to see the difference in the overall behaviour of the process's trajectories when the chosen parameters change.

4.1.2 Simulation of the CIR and Integrated CIR Processes

There is another process involved in the simulation of the time-changed Meixner process: the integrated CIR, which is the clock. The methods utilised in this simulation were described in Section 3.3. Since the discretization is an Euler scheme, it was simple to implement, despite requiring the slight corrections described earlier.

Figure A.3 features two plots that depict a trajectory of the CIR process each, obtained by the aforementioned methods. In Figure A.3a, the utilised parameters are the ones calibrated by Schoutens, which we will use to price the call options with the time-changed Meixner process in the next part of the work. Figure A.3b follows the same logic, but with different parameters, chosen randomly by us. It is possible to see the difference in the overall behaviour of the process's trajectories when the chosen parameters change, namely the effect of the mean rate of return to the mean and the long-term mean.

The integrated CIR process associated to each one of the trajectories is obtained by the scheme in eqn. (3.3.4). In Figure A.4 we show the simulation of five such trajectories and compare them with the natural evolution of time. That shows how this process makes time stochastic, which is how we introduce stochastic volatility in the Meixner process. There are periods where time goes by faster, which will correspond to periods of high volatility, while in other periods it goes slower, corresponding to the opposite.

4.2 Simulation of the Time-Changed Meixner Process

After the preparation of all the processes involved in our model, we are now able to simulate the time-changed Meixner process. As it was mentioned before, we use the integrated CIR process as a subordinator.

Note that we already have implemented the Meixner and integrated CIR processes. So, it is finally possible to implement the time-changed Meixner process. We follow the procedure presented in Section 3.4. Similarly to what we presented for the Meixner and integrated CIR processes, Figure 1 presents two plots of simulations of the time-changed Meixner process. Figure 1a depicts trajectories that were simulated with the parameters calibrated by Schoutens which will be used in the following section, where we price some call options: $(a, b, d, \kappa, \eta, \lambda, y_0) = (0.1231, -0.5875, 3.3588, 0.5705, 1.5863, 1.9592, 1)$. The parameters in Figure 1b are different, chosen randomly by us, just to illustrate the impact of another set of parameters. In that Figure, $(a, b, d, \kappa, \eta, \lambda, y_0) = (1, 2, 3, 1, 2, 3, 1)$.

5 Pricing of Vanilla Call Options

In this section, we price some vanilla call options. Our idea is to compare the results obtained with three models: the classical Black-Scholes model, the results when we only use the Meixner process, and those when we use the time-changed Meixner process. For this type of options there is also a closed-form formula to compute their price; we will also use it in this section, for the case of the time-changed Meixner process.

Figure 1: Comparison of simulations of trajectories of the time-changed Meixner process using different parameters.

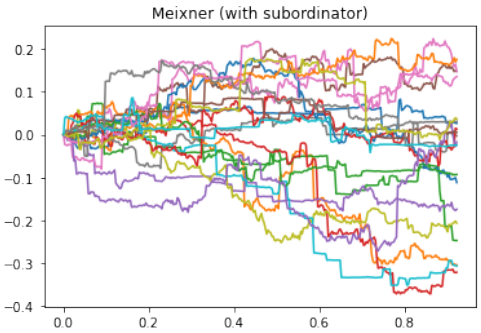

(a) Simulation of the time-changed Meixner process with the parameters calibrated by Schoutens in [8].

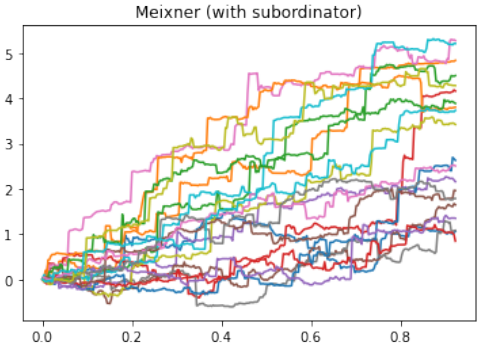

(b) Simulation of the time-changed Meixner process with randomly chosen and different parameters.

5.1 Data

The data tested on this project consists of a collection of European call option prices on the S&P 500 Index at the close of the market on 18 April 2002. It was taken from Appendix C in [8] and includes 11 close prices in USD.

These prices refer to options that expire in March 2003. It is crucial to figure out exactly what is the time to maturity that corresponds to those call options, because the day in March when those options expire is not mentioned. In spite of that, it is mentioned in [3] that in the U.S., the last day to trade an option is typically the third Friday of the expiration month, while the expiration date is the Saturday immediately afterwards. Having that said, we consider that the expiration date of these options is March 22, 2003. Therefore, the time to maturity of the options under consideration is $T = {}^{338}/_{365}$.

5.2 Closed-Form Formula

In this part of our work we are interested in computing the price of European call options. For that type of options, it is possible to derive pricing formulas in closed-form. An overview of some ways to compute European call options with such formulas is given in Schoutens's book [8].

In our work, we decided to price these call options through the characteristic function. Here, we introduce a small correction to the formula presented in [8] for the price of a call option, because of the existence of dividends. In [6], it is stated that the price of an European call option is given by:

$$C(K,T) = S_0 \exp(-qT)\Pi_1 - K\exp(-rT)\Pi_2, \tag{5.2.1}$$

where Π_1 and Π_2 are obtained by computing the integrals:

$$
\begin{aligned}
\Pi_1 &= \frac{1}{2} + \frac{1}{\pi}\int_0^\infty \mathrm{Re}\left(\frac{\exp(-\mathrm{i}u\log K)\mathbb{E}\left[\exp\left(\mathrm{i}(u-\mathrm{i})\log S_T\right)\right]}{\mathrm{i}uE\left[S_T\right]}\right)\mathrm{d}u \\
&= \frac{1}{2} + \frac{1}{\pi}\int_0^\infty \mathrm{Re}\left(\frac{\exp(-\mathrm{i}u\log K)\phi(u-\mathrm{i})}{\mathrm{i}u\phi(-\mathrm{i})}\right)\mathrm{d}u, \\
\Pi_2 &= \frac{1}{2} + \frac{1}{\pi}\int_0^\infty \mathrm{Re}\left(\frac{\exp(-\mathrm{i}u\log K)\mathbb{E}\left[\exp\left(\mathrm{i}u\log S_T\right)\right]}{\mathrm{i}u}\right)\mathrm{d}u \\
&= \frac{1}{2} + \frac{1}{\pi}\int_0^\infty \mathrm{Re}\left(\frac{\exp(-\mathrm{i}u\log K)\phi(u)}{\mathrm{i}u}\right)\mathrm{d}u.
\end{aligned}
\tag{5.2.2}
$$

The term $\exp(-qT)$ is not present in [8] but allowed us to have results with an error that is very similar to the one presented in that same reference, as we will see later. So, we decided to stick with it.

To compute the integrals in eqn. (5.2.2) we use a quadrature method already built-in in *Python*. It is capable of computing improper integrals, but probably due to the complexity of the integrating function, it was not converging. So, we decided to change the upper bound of the integral from ∞ to 1000, because we found that the result of the integral starts becoming "saturated" and converging to its result with an upper bound much lower than 1000. So, the integral with 1000 as an upper bound is a safe approximation to the improper integral.

We implemented the closed-form formula for the Meixner-CIR model. The characteristic function for the log price in that case is presented in eqn. (2.3.2).

5.3 Monte Carlo Method

For the Meixner and Meixner-CIR processes, the pricing of call options may be done by the Monte Carlo method. To the procedures described in Sections 3 and 4, we add an extra step to compute the payoff associated to each of the simulated trajectories. The payoff of a vanilla European call option is $\Phi_{\mathrm{Eur}}(x) = (x-K)^+$. Since the European call option can only be exercised at maturity, x is the stock price at maturity S_T. Then, we compute the mean of sample payoffs to get an estimate of the expected payoff. The final step is discounting the estimated payoff at the risk-free rate to get an estimate of the value of the derivative.

When Monte Carlo simulations are utilized to derive the prices of derivatives, it should be under the equivalent martingale measure $\mathbb{Q}$. In a Lévy market there are many different equivalent martingale measures to choose.

In the case of the Meixner process, one way to obtain an equivalent martingale measure is by mean-correcting the exponential of a Lévy process. This can be done by a special parameter m_{new}. In terms of the original process $\bar{X}$, this means a term $m_{\mathrm{new}}t$ is added to the process. That is reflected in the first parameter of the Lévy triplet, which will be equal to $\gamma = \bar{\gamma} + m_{\mathrm{new}}$. In the case of the Meixner distribution, that parameter is shown in [8] to be:

$$
m_{\mathrm{new}} = r - q - 2d\left[\log(\cos(b/2)) - \log(\cos((a+b)/2))\right]. \tag{5.3.1}
$$

In that case, we get that the stock price process under the risk-neutral measure $\mathbb{Q}$ is:

$$
S_t = S_0\exp(m_{\mathrm{new}}t + X_t). \tag{5.3.2}
$$

In the Meixner model with stochastic volatility, the risk-neutral price process S is modelled as:

$$S_t = S_0 \frac{\exp((r-q)t)}{\mathbb{E}[\exp(X_{Y_t}) \mid y_0]} \exp(X_{Y_t}), \tag{5.3.3}$$

where X_{Y_t} is the time-changed Meixner process. By the same logic as before, the factor

$$\frac{\exp((r-q)t)}{\mathbb{E}[\exp(X_{Y_t}) \mid y_0]}$$

puts us into the risk-neutral world by the same mean-correcting argument.

For the simulations, we used 1000 simulations with 200 equally small time steps. About the chosen number of simulations, we found it was a reasonable trade-off between the time it takes to simulate the trajectories for these 11 call options with different strike prices and the standard error when using the Monte Carlo method. This decision was made with the information in Figure 9.2 in Schoutens's book [8]. The decrease in the standard error we would get by adding an order of magnitude to our number of simulations is not worth the extra 3 hours it would take to estimate these prices.

5.4 Black-Scholes Formula

In 1968, the economists Fischer Black, Myron Scholes and Robert Merton introduced the world to what would later be known as the Black-Scholes model. It is a mathematical model that, while using several unrealistic assumptions, is useful to price derivatives in financial markets. The Black-Scholes-Merton formula for the price $C(K,T)$ of an European call option at time zero with dividend yield q is given by:

$$C(K,T) = C = \exp(-qT) S_0 \mathcal{N}(d_1) - K \exp(-rT) \mathcal{N}(d_2) \tag{5.4.1}$$

where

$$\begin{aligned} d_1 &= \frac{\log(S_0/K) + \left(r - q + \frac{1}{2}\sigma^2\right) T}{\sigma\sqrt{T}}, \\ d_2 &= \frac{\log(S_0/K) + \left(r - q - \frac{1}{2}\sigma^2\right) T}{\sigma\sqrt{T}} = d_1 - \sigma\sqrt{T}, \end{aligned} \tag{5.4.2}$$

and $\mathcal{N}(x)$ denotes the cumulative probability distribution function of a standard normal random variable.

The Black-Scholes formula has several limitations. In financial markets, these limitations are critical, being that asset price processes have jumps, the distribution of asset returns is not Normal being that it exhibits fat tails and skewness.

For our simulation, we have applied $\sigma = 0.1812$. According to the book of Schoutens [8], this value gives us the best fit in the least-squared sense for the model. It was calibrated by pricing European call options on the S&P500 index between 1970 and 2001. Throughout the book, namely when pricing exotic options, Schoutens often changes this parameter. However, we have decided to maintain the same value, because it represents the risk associated with the price changes of a security. Since our data set is the same, this value must fulfil the requirements of the market in the circumstances presented. The maturity T was settled as $T = {}^{338}/_{365}$, which we explained previously.

5.5 Implied Volatility

The Black-Scholes pricing formula has six parameters, five of which are known, observable quantities in the market. This is not the case for the volatility parameter σ. One approach around this difficulty is to estimate it by applying statistical tools to the time series data of the underlying asset. A popular alternative is to infer the value of σ which the market has priced into a given option. In other words, we wish to find σ for which the Black-Scholes formula's predicted price coincides with the market value of the option. Such a value for σ is the *implied volatility* of the underlying.

There is no closed formula for extracting the implied volatility [8], hence it must be estimated using numerical methods. This can be done as follows: consider an European call option with strike K and maturity T trading for a value of $\tilde{C}$. We wish to numerically solve the transcendental equation

$$\tilde{C} = C(\sigma)$$

where $C(\sigma)$ is the map $\sigma \mapsto C(T, K)$ obtained by taking σ as a variable while holding T and K fixed in eqn. (5.4.1). We then apply the Newton-Raphson iteration procedure, starting with an initial estimate $\sigma_0 = 0.2$ as suggested in [8]. If we repeat this procedure for a sufficient number of options equal in all but strike price, by then plotting the corresponding implied volatilities we replicate the famous *volatility smile*, which directly contradicts the Black-Scholes assumption that σ is constant. This is one of the reasons why it's fruitful to consider alternative models where volatility behaves stochastically.

Figure 2 depicts a comparison of implied volatilities for the different models. The common "volatility smile" is not seen because there are not enough strike prices; we should have strikes with higher values to see it.

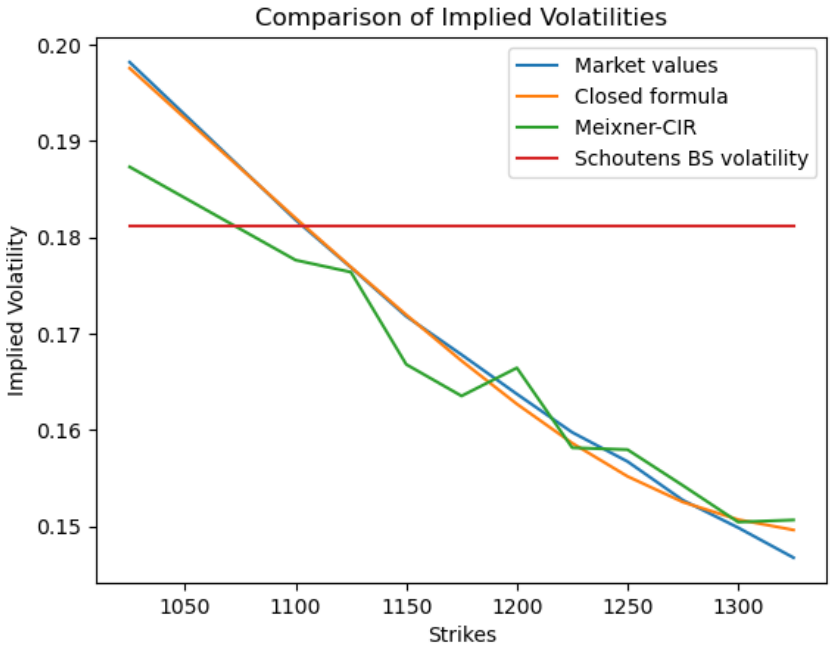

Figure 2: Implied volatilities

About the plot, since the Black-Scholes model assumes that volatility is constant, it remains in the established value throughout the different strike prices. Moreover, the closed-form formula implied volatility closely replicates the volatility smile, which is closely related to the actual prices. Finally, the Meixner-CIR process is also capable of replicating the volatility curve, but with slight deviations. It is

also not a smooth curve. This is because the pricing was performed via Monte Carlo simulations, which induces some error in the computations. It is also observed that the computed implied volatility in this case is further from the market values' curve when the options were deep in the money or deep out of the money. In fact, we observed that the model was more sensitive for those strikes, as we will explain in the following subsection.

5.6 Results and Discussion

We now see how our models perform when pricing the aforementioned call options. Table 1 depicts the estimated prices by the chosen models with the real prices.

Table 1: Comparison of real option prices (in USD) with results obtained by using the closed-form formula, the simple Meixner model, the time-changed Meixner model and the Black-Scholes formula.

Strike price	1025	1100	1125	1150	1175	1200	1225	1250	1275	1300	1325
Real prices	146.50	96.20	81.70	68.30	56.60	46.10	36.90	29.30	22.50	17.20	12.80
Closed Formula	146.12	96.11	81.55	68.21	56.17	45.66	36.31	28.59	22.33	17.37	13.51
Meixner-CIR	142.51	94.41	81.49	66.09	54.72	47.26	36.25	29.77	23.03	17.38	13.87
Meixner	149.13	94.49	85.21	66.51	58.43	47.69	39.47	29.64	24.15	19.90	14.70
BS formula	137.61	92.80	80.41	69.26	59.31	50.50	42.77	36.02	30.18	25.16	20.87

It is important to mention that in order to obtain relevant results for the time-changed Meixner model, we had to improve our approximations: we required the process to be approximated by 300 independent Poisson processes and the Monte Carlo simulations were performed with 2000 trajectories. We were forced to do this, particularly in the cases when the options were deep in the money or deep out of the money. This model revealed itself to be very sensitive for those strike prices.

Moreover, in order to compare our results, we have computed the average relative percentage error (ARPE), as suggested in the book of Schoutens [8]:

$$\text{ARPE} = \frac{1}{\text{number of options}} \sum_{\text{options}} \frac{|\ \text{market price} - \text{model price}\ |}{\text{market price}} \tag{5.6.1}$$

We summarize the obtained results in the following Table 2.

Table 2: Average Related Percentage Error comparison.

	Closed Formula	**Meixner-CIR**	**Meixner**	**BS Formula**
ARPE	1.18%	2.59%	5.74%	19.02%

The data present in Table 2 leads us to conclude what was already established by the comparison of real option prices in Table 1. The most appropriate way to price these vanilla European call options was via closed-form formula. This was already expected, as no randomness takes part in the computation of the prices in that case. No matter how many simulations are performed in the Monte Carlo method, there is always an error present that will be intrinsic to that methodology, and so it was expected *a priori* that those estimates would result in worse approximations to reality.

As for the Monte Carlo approximations, the model with best results is, all things considered, the time-changed Meixner. Furthermore, the Meixner model revealed to be a pretty good competitor to

the more sophisticated model with stochastic volatility. It should also be noted that, as expected, the Black-Scholes formula yielded results that are not a good approximation of reality.

It is possible to interpret these results under the light of Finance theory. Overall, the estimates with highest errors were obtained with the Black-Scholes formula. The strongest underlying assumption in that model is that returns are log-normally distributed, but there are other assumptions, such as the non-existence of jumps in the stock price. It is a stylized fact of financial returns that extreme events can occur with a higher probability than is expected from a Gaussian distribution, and so log returns are not normally distributed. Hence, the Black-Scholes formula is a poor approximation of financial data. With the Meixner model, we introduce fat tails in the distribution of returns (as the kurtosis becomes greater than 3) and jumps in the stock price are allowed. So, option pricing with this model gives better results. The Meixner-CIR model is an upgrade to both models. The randomness of the CIR process introduces stochastic volatility in the model, and the mean reversion induces volatility clustering. This has a translation in Finance: volatility changes randomly across time, but tends to cluster: on one hand, a short period of high volatility tend to be followed by another short period of high volatility, and on the other hand, when in a certain period the market is "calmer", it is expected to remain in that state over the following period.

However, we observe that the ARPE we obtained for the Meixner-CIR model is higher than the one presented by Schoutens. We highlight the following reasons for that:

1. The value for the ARPE statistic presented by Schoutens in [8] was computed for the entire dataset which comprises 77 call options with different times to maturity. So, the model could very well be underperforming in the case of the options that expire in March 2003 when compared to the remaining maturities;

2. Not only was the ARPE computed for the whole dataset, but also the parameters we used were also calibrated for all the options available. The parameters calibrated by Schoutens may not be the best fit to the specific time to maturity we worked with, which could yield higher errors;

3. Furthermore, the Meixner-CIR model is not as parsimonious as the Meixner model, as it contains more parameters. Therefore, an unoptimized set of parameters can worsen the model's fit quite dramatically.

6 Pricing of an Exotic Option

In this part of the work, we estimate the price of an exotic barrier option of the type "down-and-in barrier call" (DIBC). This option is a standard European call with strike K if its minimum goes below some low barrier H. If this barrier is never reached during the lifetime of the option, the option expires worthless. Its initial price is given by:

$$\text{DIBC} = \exp(-rT)\mathbb{E}^{\mathbb{Q}}\left[(S_T - K)^+ \mathbf{1}_{m_T^S \leq H}\right] \tag{6.0.1}$$

where m_T^S is the minimum price attained during the entire lifespan of the option.

To price this option, we will use both the Meixner and the Meixner-CIR models. Moreover, it is requested to price a DIBC with the following characteristics: $T = 9/12, K = S_0 = 1124.47$, and

$H = 0.95 \times S_0 = 1068.2465$. However, in Schoutens's book we have the prices computed for the same exotic option but with a different time to maturity ($T = 1$).

Pricing of a DIBC with time to maturity of 1 year

Therefore, we will start by computing the price of the DIBC with the same parameters as in Schoutens, to have some sense on whether our estimate is good. Only then, having the certainty that our algorithm is implemented correctly, we proceed to price the DIBC with the requested time to maturity, $T = 9/12$.

The following Table 3 presents the value obtained for the aforementioned exotic option by Schoutens in [8] with our two estimates: one with the time-changed Meixner model, and the other one with the simple Meixner model. These estimates were computed with the Monte Carlo method. We considered the approximation with 300 Poisson processes and 5000 simulations.

Table 3: Comparison of the DIBC prices obtained with different models.

	Meixner-CIR in [8]	**Meixner-CIR**	**Meixner**
Price (in USD)	17.24	18.62	8.70

The value we obtained for the given option is similar to that obtained by Schoutens when we use the Meixner-CIR. However, there is a small error associated to our computation, which may be due to the reasons mentioned before, in the previous Section.

There is an important conclusion to be drawn from these results. Note that, for the pricing of call options, the Meixner model was a good approximation of reality. However, it reveals big shortcomings when pricing the DIBC under consideration. Its error was above 100%, and so the Meixner model is inadequate for the pricing of this exotic option.

Pricing of a DIBC with time to maturity of 9 months

Now, we proceed to the estimate of the price of a DIBC with time to maturity of 9 months, using the Meixner-CIR model. Recall, this is the DIBC with $T = 9/12, K = S_0 = 1124.47$, and $H = 0.95 \times S_0$.

Again, we considered the approximation with 300 Poisson processes and 5000 simulations. The value we obtained for the price of the DIBC was **15.42 USD**.

7 Conclusions

The project's purpose was to explore the application of stochastic volatility models in option pricing in order to obtain estimations that would be more exact than with regular models.

Based on the obtained results, it is possible to conclude that the Meixner-CIR is the most accurate model to price options, followed by the Meixner process with deterministic time. As expected, as we relaxed the assumptions of the Black-Scholes model, the results got progressively better. First, by allowing for jumps in the stock price and by introducing heavy tails with the Meixner model, we were able to price vanilla call options with good accuracy, although that model revealed its shortcomings when pricing an exotic option. Those problems were surpassed with the introduction of stcohastic volatility, which

induces some stylized facts of financial returns in the model; namely, that volatility changes stochastically and that it tends to cluster.

The initial goal of our project was fulfilled, being that we were able to demonstrate the importance of developing an accurate characterization of financial markets while reducing assumptions. Even though our objectives were accomplished, we obtained a higher value for the ARPE statistic than the one presented by Schoutens, which can be justified by a different dataset and a different set of parameters, as explained before.

Overall, this project allowed us to explore in depth financial modelling and provided us a deeper understanding of the different obstacles one may encounter in doing so. The weeks dedicated to experimenting and tailoring the models provided us a great introduction to the complex algorithms employed in the field, and the importance of the intersection between advanced numerical methods and financial knowledge.

References

[1] Leif BG Andersen, Peter Jäckel, and Christian Kahl. Simulation of square-root processes. *Encyclopedia of Quantitative Finance*, pages 1642–1649, 2010.

[2] Peter Carr, Hélyette Geman, Dilip B Madan, and Marc Yor. Stochastic volatility for Lévy processes. *Mathematical finance*, 13(3):345–382, 2003.

[3] Akhilesh Ganti. Expiration time explained: What it is, how it works, example, 2022.

[4] Dilip B Madan, Peter P Carr, and Eric C Chang. The variance gamma process and option pricing. *Review of Finance*, 2(1):79–105, 1998.

[5] Benoit B. Mandelbrot. *Fractals and scaling in finance: Discontinuity, concentration, risk*. Springer Science & Business Media, 2013.

[6] Rui Monteiro. Option Pricing with Lévy Processes: Jump models for European-style options. Master's thesis, ISCTE-IUL, Instituto Universitário de Lisboa, 2013.

[7] Wim Schoutens. *The Meixner process: Theory and applications in finance*. Eurandom Eindhoven, 2002.

[8] Wim Schoutens. *Lévy processes in finance: pricing financial derivatives*. John Wiley & Sons, Ltd, 2003.

[9] Wim Schoutens and Jozef L Teugels. Lévy processes, polynomials and martingales. *Stochastic Models*, 14(1-2):335–349, 1998.

A Appendix

Figure A.1: Comparison of the intensity parameters λ_i obtained in our and Schoutens's implementations.

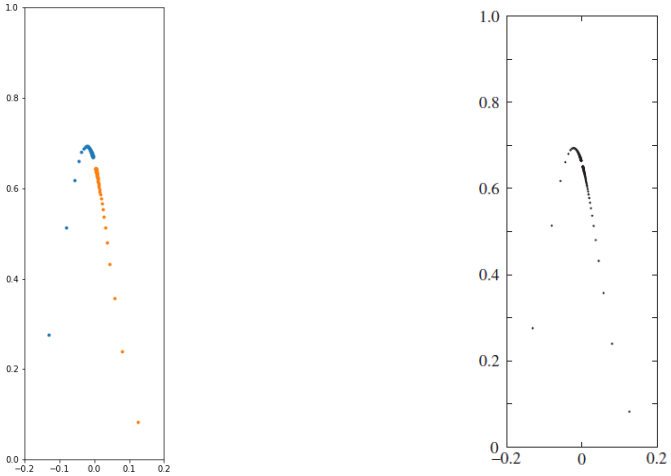

(a) The plot obtained in our implementation. (b) The plot obtained by Schoutens in [8].

Figure A.2: Comparison of simulations of twenty trajectories of the Meixner Process using different parameters.

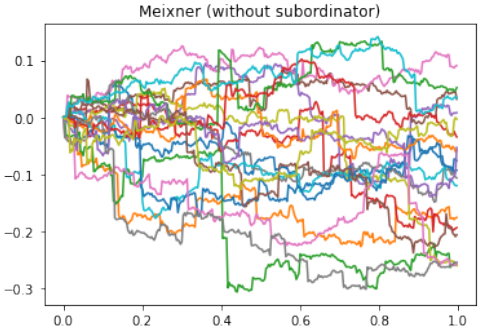

(a) Simulation of the Meixner process with the parameters calibrated by Schoutens in [8]: $a = 0.3977, b = -1.4940, d = 0.3462$

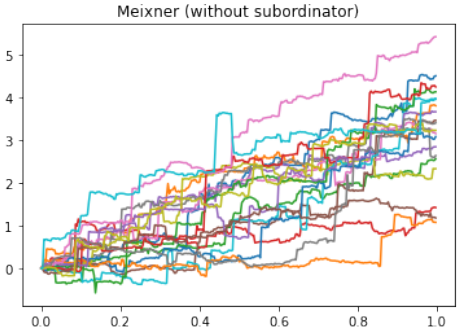

(b) Simulation of the Meixner process with randomly chosen and different parameters: $a = 1, b = 2, d = 3$

Figure A.3: Comparison of simulations of trajectories of the CIR Process using different parameters.

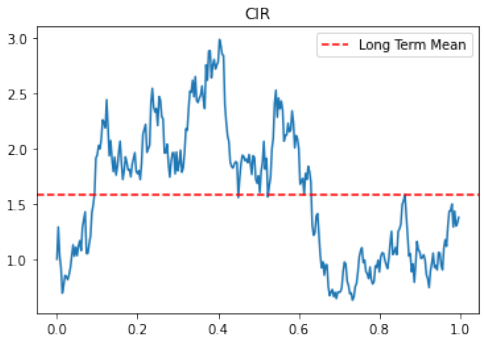

(a) Simulation of the CIR process with the parameters calibrated by Schoutens in [8]: $\kappa = 0.5705, \eta = 1.5863, \lambda = 1.9592, y_0 = 1$

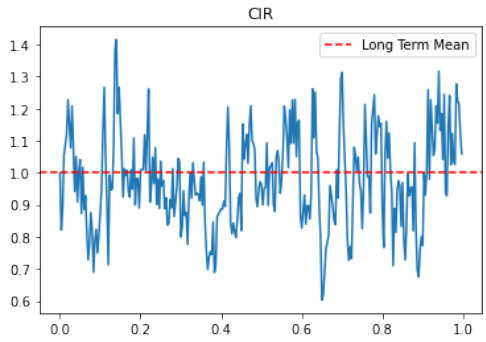

(b) Simulation of the CIR process with randomly chosen and different parameters: $\kappa = 100, \eta = 1, \lambda = 2, y_0 = 1$

Figure A.4: Comparison of the natural time and five trajectories of the Integrated CIR Process.